Preprints of the 21st IFAC World Congress (Virtual)
Berlin, Germany, July 12-17, 2020

Synchronization in networks of systems with synchronous/asynchronous sampled-data couplings ⋆

Kanako Sakai * **Iori Yoshida** * **Toshiki Oguchi** *

* *Graduate School of Systems Design, Tokyo Metropolitan University, 1-1, Minami-Osawa, Hachioji-shi, Tokyo 192-0397 Japan (e-mail: tmu.sakai@gmail.com, yoshida-iori@ed.tmu.ac.jp, t.oguchi@tmu.ac.jp).*

Abstract: This paper considers the network synchronization problem of nonlinear systems with sampled-data couplings. In particular, we focus on sufficient conditions for full synchronization of systems interconnected via sampled-data couplings. We have already derived a sufficient condition for synchronization of two mutual coupled systems whose outputs are simultaneously measured with the same constant sampling interval. By extending the result, in this paper, we show that the network synchronization condition can be estimated from that of two coupled systems by scaling the stability region with a factor related to the eigenvalues of the graph Laplacian. Furthermore, we discuss the effect of asynchronous sampling on synchronization. The validity of the obtained results is illustrated by numerical simulations.

Keywords: synchronization, sampled-data systems, networks, synchronous sampling, asynchronous sampling

1. INTRODUCTION

Synchronization of nonlinear systems, including chaotic systems, is still now a hot topic in the interdisciplinary fields such as applied physics, applied mathematics, mathematical biology, social sciences, and control engineering(Pikovsky et al. (2003), Strogatz (2012)). In particular, synchronization in networks of nonlinear systems is closely connected to cooperative control of multi-agent systems (Olfati-Saber et al. (2007)) such as the consensus and formation control problems of mobile robots and unmanned aerial vehicles. Therefore, synchronization problems have been widely investigated, ranging from the master-slave synchronization to network synchronization, from static couplings to delayed couplings and dynamical couplings in a field of control science. Most of these studies treated couplings that are realized as continuous-time couplings. In many real-world applications, however, systems are not always connected via continuous-time couplings. Artifacts such as networked systems with computer network technology are constructed by interconnecting systems via sampled-data communication. Therefore, synchronization problems of sampled-data systems have also been investigated in recent years, and several conditions for the master-slave synchronization based on sampled-data are proposed with different approaches. Nevertheless, in networks of nonlinear systems, the relationship among the sampling period, coupling strength and synchronization is not well understood.

In our previous work (Sakai and Oguchi (2019)), we considered the synchronization problem of two mutual coupled systems via synchronous sampled-data couplings. As a result, we derived a sufficient condition for synchronization as a relationship between the coupling strength and the sampling interval. Furthermore, the obtained condition is similar to the synchronization condition for systems with delayed couplings (Steur and Nijmeijer (2011)). In this paper, we consider the synchronization problem in networks of systems interconnected via sampled-data couplings. First, we briefly review our previous results, and then we consider the network synchronization of systems with an undirected graph topology. Finally, we also discuss the effect of asynchronous sampling on synchronization. As a result, the network systems connected via asynchronous sampled-data couplings cannot accomplish perfect synchronization, but it can accomplish synchronization in the sense of practical synchronization.

2. PROBLEM SETTINGS

We consider N identical nonlinear systems defined as follows. For $i = 1, \ldots, N$,

$$\Sigma_i : \begin{cases} \dot{x}_i(t) = A_0 x_i(t) + f(x_i(t)) + B u_i(t) \\ y_i(t) = C x_i(t), \end{cases} \tag{1}$$

where $x_i \in \mathbb{R}^n, u_i, y_i \in \mathbb{R}^m$ are the state, the input, and the output, respectively. Moreover, $f(\cdot) : \mathbb{R}^n \to \mathbb{R}^n$ is a sufficiently smooth vector field, and A_0, B and C are constant matrices with appropriate dimensions. In addition, we assume that $CB =: b \in \mathbb{R}^{m\times m}$ is positive definite. Under this assumption, systems (1) can be transformed into

$$\overline{\Sigma}_i : \begin{cases} \dot{z}_i(t) = q(z_i(t), y_i(t)) \\ \dot{y}_i(t) = a(z_i(t), y_i(t)) + b u_i(t) \end{cases} \tag{2}$$

⋆ This study is partially supported by JSPS KAKENHI Grant number JP17K06503.

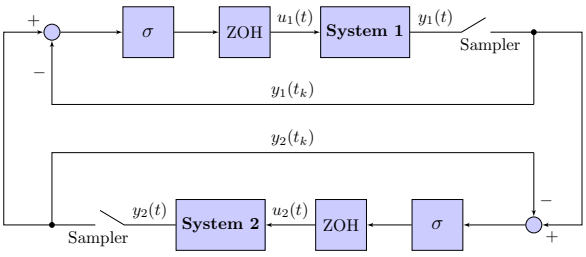

Fig. 1. Bidirectional sampled-data coupling.

for $i = 1, \ldots, N$, where $z_i \in \mathbb{R}^{n-m}, u_i, y_i \in \mathbb{R}^m, q(\cdot,\cdot) : \mathbb{R}^n \to \mathbb{R}^{n-m}$, and $a(\cdot,\cdot) : \mathbb{R}^n \to \mathbb{R}^m$. Throughout this paper, $\|\cdot\|$ denotes the Euclidean norm.

Furthermore, we assume that the following two assumptions hold.

Assumption 1. Each system (1) is strictly $\mathcal{C}^1$-semi-passive, i.e., for any initial state $x_i(t_0)$, there exists a radially unbounded positive definite storage function $V \in \mathcal{C}^1(\mathbb{R}^n, \mathbb{R}_{\geq 0})$ such that

$$\dot{V}(x_i(t)) \leq y_i^\top(t) u_i(t) - H(x_i(t)) \tag{3}$$

where $H(\cdot) : \mathbb{R}^n \to \mathbb{R}$ is a scalar positive function outside some ball $\mathcal{B} = \{x_i(t) : \|x_i(t)\| < \rho\}$ with the constant $\rho > 0$:

$$\exists \rho > 0, \forall \|x_i(t)\| \geq \rho \Rightarrow H(x_i(t)) \geq \varrho(\|x_i(t)\|)$$

for some continuous positive function $\varrho(\|x_i(t)\|)$ defined for $\|x_i(t)\| \geq \rho$.

Assumption 2. For the sub-dynamics $\dot{z}_i(t) = q(z_i(t), y_i(t))$ in each system (2), there exist a positive definite function $V_0 \in \mathcal{C}^2(\mathbb{R}^{n-m}, \mathbb{R}_{\geq 0})$ and a positive constant α such that

$$\nabla V_0^\top(\overline{z}_{ij}(t))(q(z_i(t), y^*(t)) - q(z_j(t), y^*(t))) \leq -\alpha \|\overline{z}_{ij}(t)\|^2 \tag{4}$$

for all $z_i, z_j \in \mathbb{R}^{n-m}$ and all $y^* \in \mathbb{R}^m$, where $\overline{z}_{ij}(t) := z_i(t) - z_j(t)$.

Assumption 2 implies that $z_i(t) = z_j(t)$ is globally asymptotically stable fixing as $y_i(t) = y_j(t) = y^*(t)$. Then z_i and z_j converge to a unique solution determined by y^*.

Initially, we assume that the outputs of systems (1) are simultaneously measured at $t_k = kh$ for $k \in \mathbb{N}$ by simultaneous sampling, where $h \in \mathbb{R}_{\geq 0}$ denotes a constant sampling period. Based on the measured output $y_i(t_k)$ for $i \in \mathcal{I} = \{1, 2, \ldots, N\}$, each system is coupled with other systems via the following synchronous sampled-data couplings.

$$u_i(t) = -\sigma \sum_{j=1, j\neq i}^{N} a_{ij}(y_i(t_k) - y_j(t_k)), \quad \forall t \in [t_k, t_{k+1}) \tag{5}$$

where $\sigma \in \mathbb{R}_{>0}$ is a common constant coupling strength and a_{ij} corresponds to the (i,j)-element of the adjacency matrix A of the corresponding undirected graph $\mathcal{G}$ with N nodes to the network structure, i.e., if there exists a coupling between systems i and j, then $a_{ij} = a_{ji} = 1$, and otherwise $a_{ij} = a_{ji} = 0$. Then the network topology of the coupled system can be characterized by the graph Laplacian $L(\mathcal{G}) = D(\mathcal{G}) - A(\mathcal{G})$, where $D(\mathcal{G})$ and $A(\mathcal{G})$ are the degree matrix and the adjacency matrix of the graph $\mathcal{G}$, respectively.

Using the graph Laplacian $L(\mathcal{G})$, the input vector $u(t) = \mathrm{col}(u_1(t). \ldots, u_N(t))$ can be described by the following equation.

$$u(t) = -\sigma(L(\mathcal{G}) \otimes I_m) y(t_k)$$

where $y(t_k) = \mathrm{col}(y_1(t_k), \ldots, y_N(t_k))$, and the notation $\otimes$ denotes the Kronecker product.

This coupling means that $u_i(t)$ for each system is samplewise constant and each system is changed the input value at $t = t_k$ only. Figure 1 shows a block diagram of two systems coupled by sampled-data couplings. For the coupled systems, we define synchronization as follows. There are several definitions of synchronization (Blekhman et al. (1997)), but throughout this paper, we adopt the following definition (Pogromsky et al. (2002)).

Definition 1. Consider the systems given by Eq. (1) coupled via (5). Systems i and j under coupling (5) are said to be synchronized, if $\|e_{ij}(t)\| := \|x_i(t) - x_j(t)\| \to 0$ as $t \to \infty$ for any initial conditions $x_i(t_0)$ and $x_j(t_0)$.

Furthermore, we introduce a notion of practical synchronization.

Definition 2. Consider the systems (1) with couplings. Systems i and j under coupling (5) are said to be practically synchronized, if there exist a class $\mathcal{KL}$ function such that

$$\|e_{ij}(t)\| \leq \beta(\|x_i(t) - x_j(t)\|, 0) + \varepsilon \tag{6}$$

for any initial conditions $x_i(t_0)$ and $x_j(t_0)$, where ε is a positive number.

3. SYNCHRONIZATION OF COUPLED SYSTEMS VIA SYNCHRONOUS SAMPLED-DATA COUPLINGS

In this section, we consider synchronization conditions for networks of nonlinear systems with synchronous sampled-data couplings. We have already derived a sufficient condition (Sakai and Oguchi (2019)) for synchronization of two coupled systems with sampled-data bidirectional coupling by following a derivation procedure of synchronization condition for the conventional continuous-time coupled systems (Pogromsky et al. (2002)). In this section, we firstly introduce our previous results on synchronization of two coupled systems via sampled-data couplings, and then we consider the synchronization problem for N coupled systems.

3.1 Synchronization condition for two mutual coupled systems via synchronous sampled-data couplings

First, we consider the behaviors of coupled systems with sampled-data couplings. The following theorem guarantees the ultimate boundedness of the solution of the coupled systems. This property means that the solution enters a compact set in finite time independent of the initial conditions.

Theorem 3. (Sakai and Oguchi (2019)) Consider two identical systems (1) bidirectionally coupled by (5). Suppose that each system satisfies Assumption 1 with ρ and $H(x_i(t))$ satisfying $H(x_i(t)) - 2\sigma\|y_i(t)\|^2 > 0$ for $\|x_i(t)\| > \rho$. Then, the solution of the closed-loop system (1) with (5) is ultimately bounded.

Next, we consider the existence of synchronization manifold. In order for synchronization of two coupled systems

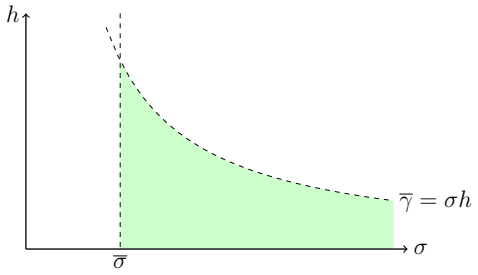

Fig. 2. Synchronization region indicated by Theorem 5.

to occur, the following linear manifold must be positively invariant for the coupled systems.

$$\mathcal{M} = \{\mathrm{col}(z_1(t), z_2(t), y_1(t), y_2(t)) \in \mathbb{R}^{2n} : z_1(t) = z_2(t) \text{ and } y_1(t) = y_2(t)\}$$

Theorem 4. (Sakai and Oguchi (2019)) The linear manifold $\mathcal{M}$ is positively invariant under the coupled systems (2) with (5). Then $\mathcal{M}$ is the synchronization manifold.

Next, we show a sufficient condition for full synchronization of the two coupled systems.

Theorem 5. (Sakai and Oguchi (2019)) Consider two systems (2) coupled bidirectionally via (5). Suppose Assumptions 1 and 2 are satisfied. Then, there exist positive constants $\overline{\sigma}$ and $\overline{\gamma}$ such that the systems (2) synchronize for any σ and h satisfying $\sigma > \overline{\sigma}$ and $\sigma h < \overline{\gamma}$.

Remark 6. Theorem 5 shows that if each system satisfies Assumptions 1 and 2, there exists always a region $\{(\sigma, h) | \sigma > \bar{\sigma} \text{ and } \sigma h < \bar{\gamma}\}$ such that if (σ, h) is in the region, then the coupled systems synchronize. Figure 2 illustrates the synchronization region with respect to the coupling strength σ and the sampling interval h as the green region. It is worth noting that the obtained synchronization region has a similar shape to the synchronization region obtained in Steur and Nijmeijer (2011) for coupled systems with delayed couplings.

3.2 Synchronization condition for N coupled systems with sampled-data couplings

Applying the input vector given by

$$u(t) = -\sigma(L(\mathcal{G}) \otimes I_m) y(t_k) = -\sigma(L(\mathcal{G}) \otimes C) x(t_k),$$

the total dynamics of the network system is described by the following equation.

$$\begin{aligned}\dot{x}(t) =& (I_N \otimes A_0)x(t) + F(x(t)) \\ & - \sigma(I_N \otimes B)(L(\mathcal{G}) \otimes C)x(t_k) \end{aligned} \tag{7}$$

where $F(t) = \mathrm{col}(f(x_1(t)), \cdots, f(x_N(t)))$.

For the above network system, we derive a synchronization condition based on the synchronization condition for two bidirectional coupled systems with synchronous sampled-data couplings.

First, we derive the error dynamics of two bidirectional coupled systems with synchronous sampled-data couplings. Defining the synchronization error between systems 1 and 2 as $e_{12}(t) = x_1(t) - x_2(t)$, the synchronization error dynamics is given by

$$\dot{e}_{12}(t) = A_0 e_{12}(t) + \psi(x_1(t), e_{12}(t)) - 2\sigma BC e_{12}(t_k) \tag{8}$$

for all $t \in [t_k, t_{k+1})$, where

$$\psi(x_1(t), e_{12}(t)) = f(x_1) - f(x_1(t) - e_{12}(t)).$$

Therefore, if the zero solution of the synchronization error dynamics of two coupled systems (8) is asymptotically stable, then synchronization of the two coupled systems is accomplished. Now, we assume that there exists a set $\{(\sigma, h)\}$ where the zero solution of the synchronization error dynamics (8) is asymptotically stable and denote the set as $\mathcal{S}$.

Next, we consider N bidirectionally coupled systems with synchronous sampled-data couplings. We define the synchronization error as

$$\begin{aligned} e(t) =& \begin{bmatrix} e_{12}(t) \\ \vdots \\ e_{1N}(t) \end{bmatrix} = \begin{bmatrix} x_1(t) - x_2(t) \\ \vdots \\ x_1(t) - x_N(t) \end{bmatrix} \\ :=& (M \otimes I_n)x(t) \end{aligned} \tag{9}$$

where $M = \begin{bmatrix} 1 & -1 & & 0 \\ \vdots & & \ddots & \\ 1 & 0 & & -1 \end{bmatrix} \in \mathbb{R}^{(N-1)\times N}$ and apply the coordinate transformation defined by

$$\begin{bmatrix} x_1(t) \\ e(t) \end{bmatrix} = \left(\left[\begin{array}{c|ccc} 1 & 0 & \cdots & 0 \\ \hline 1 & -1 & & 0 \\ \vdots & & \ddots & \\ 1 & 0 & & -1 \end{array}\right] \otimes I_n \right) x(t) := (M_0 \otimes I_n)x(t) \tag{10}$$

to the dynamics of the total systems. Then, the total system can be rewritten as

$$\begin{aligned} \begin{bmatrix} \dot{x}_1(t) \\ \dot{e}(t) \end{bmatrix} =& (I_N \otimes A_0) \begin{bmatrix} x_1(t) \\ e(t) \end{bmatrix} + \begin{bmatrix} f(x_1) \\ \Psi(x_1(t), e(t)) \end{bmatrix} \\ & - \sigma \left[\begin{array}{c|ccc} 0 & a_{12}BC & \cdots & a_{1N}BC \\ \hline 0 & & ML(\mathcal{G})M^+ \otimes BC & \end{array}\right] \begin{bmatrix} x_1(t_k) \\ e(t_k) \end{bmatrix}, \\ & \forall t \in [t_k, t_{k+1}) \end{aligned} \tag{11}$$

where $\Psi(x_1(t), e(t)) = \mathrm{col}(\psi(x_1(t), e_{12}(t)), \cdots, \psi(x_1(t), e_{1N}(t)))$, $M_0 = M_0^{-1}$, and $M^+ \in \mathbb{R}^{N\times(N-1)}$ denotes a pseudo inverse of M given by

$$M^+ = \begin{bmatrix} 0 & & \mathbf{0} \\ -1 & \ddots & \\ & \ddots & 0 \\ \mathbf{0} & & -1 \end{bmatrix} \in \mathbb{R}^{N\times(N-1)}.$$

Note that (11) consists of the dynamics of x_1 and the following synchronization error dynamics.

$$\begin{aligned} \dot{e}(t) =& (I_{N-1} \otimes A_0)e(t) + \Psi(x_1(t), e(t)) \\ & - \sigma(ML(\mathcal{G})M^+ \otimes BC)e(t_k), \forall t \in [t_k, t_{k+1}) \end{aligned} \tag{12}$$

3.3 Complete graph networks

If the network structure $\mathcal{G}$ is the complete graph with N nodes, which is denoted as K_N, the the corresponding graph Laplacian $L(K_N)$ is given by

$$L(K_N) = \begin{bmatrix} N-1 & -1 & \cdots & -1 \\ -1 & N-1 & \ddots & \vdots \\ \vdots & \ddots & \ddots & -1 \\ -1 & \cdots & -1 & N-1 \end{bmatrix},$$

and the eigenvalues are $\lambda_1 = 0$ with multiplicity 1 and $\lambda_2 = N$ with multiplicity $N-1$. Therefore, the matrix $ML(K_N)M^+$ in the third term on the right-hand side of the equation (12) is

$$ML(K_N)M^+ = \mathrm{diag}(N, \cdots, N) \in \mathbb{R}^{(N-1)\times(N-1)},$$

the synchronization error dynamics has a block-diagonal structure and is decomposed into $N-1$ identical subsystems.

$$\dot{e}_{1i}(t) = A_0 e_{1i}(t) + \psi(x_1(t), e_{1i}(t)) - N\sigma BC e_{1i}(t_k) \quad (13)$$

From this equation, we know that the synchronization condition for the network system (7) is equivalent to the stability condition of the origin of the decomposed equation (13). In addition, comparing the synchronization error dynamics (8) for $N=2$ with the equation (13) for $N=N$, we know that the stability region $\{(\sigma, h)\}$ of Eq. (13) for any $N \geq 3$ is given by scaling the synchronization region $\mathcal{S} = \{(\sigma, h)\}$ for $N=2$ with respect to the coupling strength σ. As a result, the synchronization region for an N-coupled system with synchronous sampled-data couplings with the complete graph structure can be estimated by obtaining the synchronization region $\mathcal{S}$ for $N=2$ and scaling $\mathcal{S}$ by a factor $\frac{2}{N}$ over the coupling strength σ-axis, that is, if a pair (σ, h) for the N-complete graph network satisfies $(\frac{N}{2}\sigma, h) \in \mathcal{S}$, we can estimate that all of the systems in the network are synchronized for the coupling strength σ and the sampling interval h. Based on the above discussion, we can state the following theorem.

Theorem 7. Consider N systems (1) on a complete graph network that are interacted with synchronous sampled-data couplings (5). Suppose that there exists a non-empty set $\mathcal{S}$ such that two coupled systems ($N=2$) synchronize for any $(\sigma, h) \in \mathcal{S}$. Then the $N(\geq 3)$ coupled systems (1) synchronize if $(\frac{N}{2}\sigma, h) \in \mathcal{S}$.

3.4 General network systems

Next, we consider network systems with general network topologies. The matrix $ML(\mathcal{G})M^+$ is not always diagonal and in turn the error dynamics also not, but there always exists a non-singular matrix P such that $P^{-1}ML(\mathcal{G})M^+P = \mathrm{diag}(\lambda_2, \cdots, \lambda_N)$, where λ_i are the eigenvalues of $L(\mathcal{G})$ and satisfy $0 = \lambda_1 < \lambda_2 \leq \cdots \leq \lambda_N$. Linearizing $\Psi(x_1, e)$ around $e=0$ and applying the coordinate transformation $e = (P \otimes I_n)\bar{e}$ into (12), the synchronization error dynamics can be rewritten as follows.

$$\begin{aligned}\dot{\bar{e}}(t) =& (I_{N-1} \otimes (A_0 + \psi'(x_1(t))))\bar{e}(t) \\ &- \sigma(P^{-1}ML(\mathcal{G})M^+P \otimes BC)\bar{e}(t_k), \forall t \in [t_k, t_{k+1})\end{aligned} \quad (14)$$

Since $P^{-1}ML(\mathcal{G})M^+P$ is diagonal, the equation (14) can be decomposed into $N-1$ independent equations as follows.

$$\dot{\bar{e}}_{1i}(t) = (A_0 + \psi'(x_1(t)))\bar{e}_{1i}(t) - \lambda_i \sigma BC\bar{e}_{1i}(t_k) \quad (15)$$

for $i = 2, \ldots, N$.

Now we assume that each above equation is asymptotically stable for a pair $(\sigma, h) \in \mathcal{S}_i$, where $\mathcal{S}_i$ denotes the corresponding stability region and the intersection $\bar{\mathcal{S}} = \bigcap_{i\in\mathcal{J}} \mathcal{S}_i$ is nonempty for $\mathcal{J} = \{2, \ldots, N\}$. If $(\sigma, h) \in \bar{\mathcal{S}}$, then the zero solution of the error dynamics (12) is locally asymptotically stable and eventually full synchronization in the network is accomplished. As a result, the synchronization region can be estimated by the intersection of the stability regions (σ, h) for all of the systems (15). In addition, replacing $\lambda_i\sigma$ with $\bar{\sigma}$ allows all of the systems (15) to be identified. Therefore, the synchronization region can also be estimated by scaling the synchronization region for two mutually coupled systems via sampled-data couplings depending on the eigenvalues of the graph Laplacian and seeking the intersection of all of the scaled regions.

Theorem 8. Consider N systems (1) on networks with any undirected graph topology. Assume that a pair (σ, h) is in a non-empty set $\bar{\mathcal{S}} = \bigcap_{i\in\mathcal{J}} \mathcal{S}_i$ for $\mathcal{J} = \{2, \ldots, N\}$. Then the zero solution of the synchronization error dynamics is locally asymptotically stable, and this means that full synchronization in the network is accomplished, i.e., $x_1(t) = x_2(t) = \cdots = x_N(t)$ as $t \to \infty$.

4. ASYNCHRONOUS SAMPLED-DATA COUPLINGS

In this section, we consider networks of systems with asynchronous sampled-data couplings. In particular, we focus on the effect of asynchronous sampling on synchronization.

For simplicity of discussion, we consider two mutual coupled systems with asynchronous sampled-data couplings. We assume that the outputs of systems 1 and 2 are measured at sampling instants t_k and $t_k^\Delta = t_k + \Delta_h$, respectively, where $\Delta_h \in [0, h)$ denotes the difference between the sampling instants for the two systems. Then the input with zero-order hold for each system is given as follows.

$$\begin{cases} u_1(t) = -\sigma(y_1(t_k) - y_2(t_{k-1}^\Delta)) \\ u_2(t) = -\sigma(y_2(t_{k-1}^\Delta) - y_1(t_k)) \end{cases}, \forall t \in [t_k, t_k^\Delta) \quad (16)$$

$$\begin{cases} u_1(t) = -\sigma(y_1(t_k) - y_2(t_k^\Delta)) \\ u_2(t) = -\sigma(y_2(t_k^\Delta) - y_1(t_k)) \end{cases}, \forall t \in [t_k^\Delta, t_{k+1}) \quad (17)$$

Using the Newton's law and the mean value theorem, these inputs can be rewritten as

$$\begin{cases} u_1(t) = -\sigma(y_1(t_k) - y_2(t_k)) - \sigma\Delta(t) \\ u_2(t) = -\sigma(y_2(t_k) - y_1(t_k)) + \sigma\Delta(t) \end{cases} \quad (18)$$

where

$$\Delta(t) = \begin{cases} (h - \Delta_h)\dot{y}_2(t_{k-1}^\Delta + \delta) & (t_k \leq t < t_k^\Delta) \\ -\Delta_h \dot{y}_2(t_k + \delta') & (t_k^\Delta \leq t < t_{k+1}) \end{cases} \quad (19)$$

and $\delta \in (0, h - \Delta_h]$, $\delta' \in (0, \Delta_h]$. Here $\Delta(t)$ is a step-like function. Under the inputs (16),(17), the synchronization error dynamics between two systems is given by

$$\begin{aligned}\dot{e}_{12}(t) =& A_0 e_{12}(t) + \psi(x_1(t), e_{12}(t)) - 2\sigma BC e_{12}(t_k) \\ &- 2\sigma BC\Delta(t).\end{aligned}$$

Therefore, the effect of asynchronous sampling appears on the synchronization error dynamics as the perturbation, and the synchronization error dynamics does not have an equilibrium point at the origin.

Theorem 9. Consider two systems (1) (or equivalently (2)) via the asynchronous sampled-data couplings (16) and (17). Under Assumptions 1 and 2, there exist positive constants $\overline{\sigma}$ and $\overline{\gamma}$ such that the systems practically synchronize for any σ and h satisfying $\sigma > \overline{\sigma}$ and $\sigma h < \overline{\gamma}$.

Due to the limitation of the space, we do not show the proof, but by reducing the synchronization problem to the practical stability problem of the synchronization error dynamics with perturbation, we derive this theorem. The

proof itself is almost the same as the proof of Theorem 5. First, we consider the behavior of the synchronization error dynamics in the interval $[t_k, t_{k+1})$. Then we show that the synchronization error converges to the bounded ball around the origin and the inequality (6) holds by using the Lyapunov-Krasovskii approach and the comparison theorem between a Krasovskii functional defined for each sampling interval and a continuous Krasovkii functional defined for all $t \geq 0$.

5. NUMERICAL EXAMPLES

In this section, we show the validity of the results obtained herein through numerical simulations of the Hindmarsh-Rose neuron systems. The Hindmarsh-Rose neuron system is given by the following mathematical model.

$$\begin{aligned}\dot{y}_i(t) =& -ay_i^3(t) + by_i^2(t) + z_{i,1}(t) - z_{i,2}(t) \\ &+ E_m + u_i(t) \\ \dot{z}_{i,1}(t) =& c - dy_i^2(t) - z_{i,1}(t) \\ \dot{z}_{i,2}(t) =& r(s(y_i(t) + Q) - z_{i,2}(t))\end{aligned}$$

where $a = 1$, $b = 3$, $c = 1$, $d = 5$, $r = 0.005$, $s = 4$, $Q = 1.618$ and $E_m = 3.25$. Under these parameters and $u_i(t) \equiv 0$, this system behaves chaotically. In addition, note that this system satisfies Assumptions 1 and 2 as shown in Oud and Tyukin (2004).

Throughout this section, we consider Hindmarsh-Rose neuron systems coupled via bidirectional sampled-data couplings with sampling interval h. In addition, the initial conditions for each system are randomly given in the range of $[0, 1]$ throughout all of the numerical examples in this section.

5.1 Synchronous sampled-data couplings

First, we clarify the synchronization condition consisting of the possible pairs of the coupling strength and the sampling interval to achieve the synchronization of two coupled systems. Figure 3 shows the synchronization errors obtained by numerical simulations in the region of $\sigma \in [0, 4]$ and $h \in (0, 10]$. In this figure, the color of each cell corresponds to the maximum value of the synchronization error between the systems for $t \in [4750, 5000]$, which is calculated by

$$c(\sigma, h) = \max_{t\in[4750,5000]} \|e_{12}(t)\| = \max_{t\in[4750,5000]} \|x_1(t) - x_2(t)\|.$$

Therefore, the dark-blue region indicates that the synchronization error is almost close to zero, and the region can be recognized as the synchronization region for this coupled system. From this figure, we can see that the sampled-data coupled systems synchronize for a larger coupling strength σ than a certain threshold value depending on sampling interval h. Compared with Figure 2, the synchronization region shown in Figure 3 is very similar in shape.

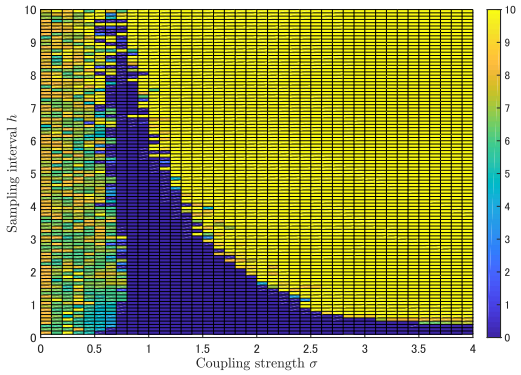

Fig. 3. Maximum synchronization error for each (σ, h).

Next, based on this simulation result, we show the validity of Theorems 7 and 8. First, we consider the complete graphs with $N = 2, 3, 4$ nodes as shown in Figure 4. If Theorem 7 holds, then the scaled region determined by scaling the synchronization region for N coupled systems with a factor $\frac{2}{N}$ over the σ-axis must coincide with the synchronization region $\mathcal{S}$ for two coupled systems. Figure 5 shows the scaled regions obtained by scaling the synchronization regions for $N = 3$ and 4 with $\frac{2}{N}$ over the σ-axis and the synchronization region for $N = 2$. These regions almost coincide, and this result illustrates the validity of Theorem 7.

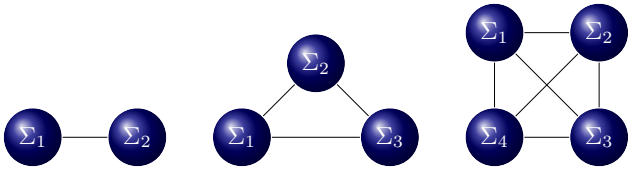

Fig. 4. Complete graphs with $N = 2, 3$, and 4 nodes

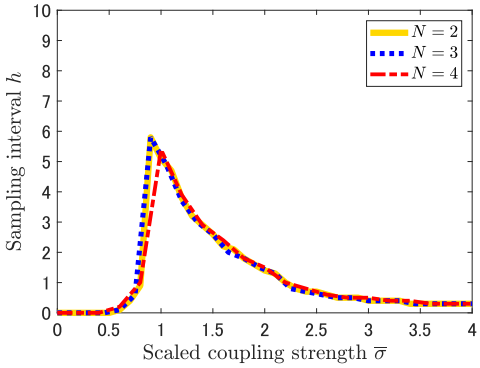

Fig. 5. Scaled synchronization regions for $N = 3$ and 4 and the synchronization region for $N = 2$.

Next, to show the validity of Theorem 8, we consider a path graph with three nodes $\mathcal{P}_3$ as shown in Figure 6. The corresponding graph Laplacian is

$$L(\mathcal{P}_3) = \begin{bmatrix} 1 & -1 & 0 \\ -1 & 2 & -1 \\ 0 & -1 & 1 \end{bmatrix}$$

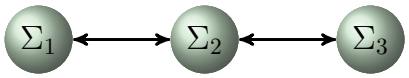

Fig. 6. Path graph with $N = 3$ nodes

and the eigenvalues are $0, 1, 3$. Now, we attempt to estimate the synchronization region by applying Theorem 8. In Figure 7, the red dotted line indicates the scaled region by scaling the synchronization region for two coupled systems with a factor $\frac{\lambda_{\min}}{2}$ over the σ-axis, and the blue dashed line indicates the scaled region corresponding to $\lambda_{\max}$, where $\lambda_{\min}$ is the nonzero minimum eigenvalue of $L(\mathcal{P}_3)$, i.e. $\lambda_{\min} = 1$, and $\lambda_{\max}$ is the maximum eigenvalue, $\lambda_{\max} = 3$. Therefore, the intersection of these two scaled regions is the estimated synchronization region for the systems on the $\mathcal{P}_3$ network. On the other hand, the black solid line indicates the synchronization region for the network system obtained through numerical simulations. The black line is completely overlapped with the estimation. Therefore, this result indicates the effectiveness of the estimation method of the synchronization region for general network systems based on Theorem 8.

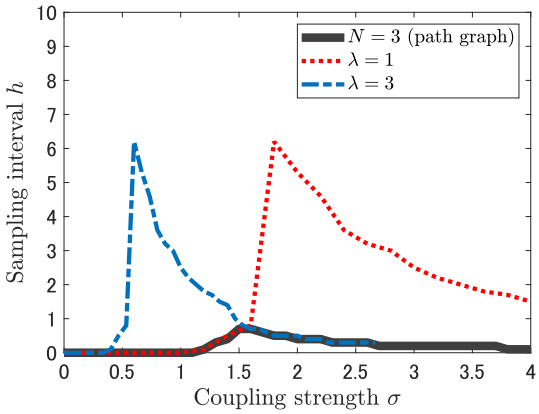

Fig. 7. Synchronization region for the 3-path graph network and the region estimated by the proposed method.

5.2 Asynchronous sampled-data couplings

At last, we consider the effect of asynchronous sampled-data couplings on synchronization. Here, we consider two mutual coupled systems via asynchronous sampled-data couplings. Fixing the time difference between samplings at two systems as $\Delta_h = t_k^{\Delta} - t_k = 0.05$, the maximum synchronization error for each (σ, h) is shown in Figure 8, which is the counterpart of Figure 3 for asynchronous sampled-data couplings with $\Delta_h = 0.05$. Due to the effect of asynchronous sampling, synchronization cannot be completely accomplished, but the synchronization error remains in the neighborhood of the origin.

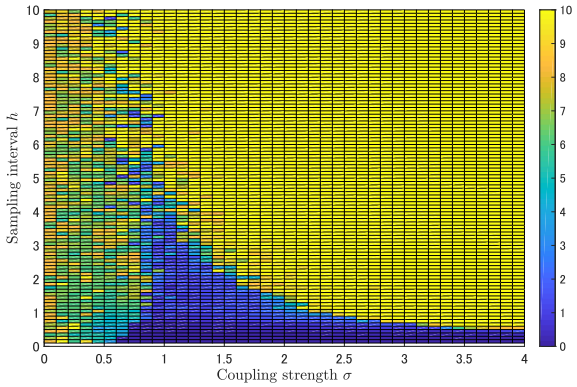

Fig. 8. The maximum synchronization error for each (σ, h) with $\Delta_h = 0.05$.

6. CONCLUSION

In this paper, we considered the synchronization problem of coupled systems via sampled-data couplings. After a brief review of our previous results, we showed that the synchronization conditions in networks of systems with undirected graph structures via synchronous sampled-data couplings can be estimated by scaling the synchronization condition obtained for two mutual coupled systems. We then investigated the synchronization problem of systems with asynchronous sampled-data couplings. For asynchronous sampled-data couplings, we discussed the problem from the viewpoint of practical synchronization.

REFERENCES

Blekhman, I., Fradkov, A., Nijmeijer, H., and Pogromsky, A.Y. (1997). On self-synchronization and controlled synchronization. *Systems & Control Letters*, 31(5), 299–305.

Olfati-Saber, R., Fax, J.A., and Murray, R.M. (2007). Consensus and cooperation in networked multi-agent systems. *Proceedings of the IEEE*, 95(1), 215–233.

Oud, W.T. and Tyukin, I. (2004). Sufficient conditions for synchronization in an ensemble of Hindmarsh and Rose neurons: Passivity-based approach. *IFAC Proceedings Volumes*, 37(13), 441–446.

Pikovsky, A., Rosenblum, M., and Kurths, J. (2003). *Synchronization: A Universal Concept in Nonlinear Sciences*. Cambridge Nonlinear Science Series. Cambridge University Press.

Pogromsky, A., Santoboni, G., and Nijmeijer, H. (2002). Partial synchronization: from symmetry towards stability. *Physica D : Nonlinear Phenomena*, 172(1-4), 65–87.

Sakai, K. and Oguchi, T. (2019). Synchronization of coupled nonlinear systems with bidirectional sampled-data couplings. *IFAC-PapersOnLine*, 52(16), 634–639.

Steur, E. and Nijmeijer, H. (2011). Synchronization in networks of diffusively time-delay coupled (semi-)passive systems. *IEEE Transactions on Circuits and Systems I: Regular Papers*, 58(6), 1358–1371.

Strogatz, S. (2012). *Sync: How Order Emerges From Chaos In the Universe, Nature, and Daily Life*. Hyperion.